ORIGINAL RESEARCH

American Heart Association | American Stroke Association

Interplay Between the Effects of Dilated Cardiomyopathy Mutation (R206L) and the Protein Kinase C Phosphomimic (T204E) of Rat Cardiac Troponin T Are Differently Modulated by α- and β-Myosin Heavy Chain Isoforms

John Jeshurun Michael, PhD; Murali Chandra, PhD

***Background*—**We hypothesized that the functional effects of R206L—a rat analog of the dilated cardiomyopathy (DCM) mutation R205L in human cardiac troponin T (TnT)—were differently modulated by myosin heavy chain (MHC) isoforms and T204E, a protein kinase C (PKC) phosphomimic of TnT. Our hypothesis was based on two observations: (1) α- and β-MHC differentially influence the functional effects of TnT; and (2) PKC isoforms capable of phosphorylating TnT are upregulated in failing human hearts.

***Methods and Results*—**We generated 4 recombinant TnT variants: wild type; R206L; T204E; and R206L+T204E. Functional effects of the TnT variants were tested in cardiac muscle fibers (minimum 14 per group) from normal (α-MHC) and propylthiouracil-treated rats (β-MHC) using steady-state and dynamic contractile measurements. Notably, in α-MHC fibers, Ca^{2+}-activated maximal tension was attenuated by R206L (≈32%), T204E (≈63%), and R206L+T204E (≈64%). In β-MHC fibers, maximal tension was unaffected by R206L, but was attenuated by T204E (≈33%) and R206L+T204E (≈40%). Thus, β-MHC differentially counteracted the attenuating effects of the TnT variants on tension. However, in β-MHC fibers, R206L+T204E attenuated tension to a greater extent when compared to T204E alone. In β-MHC fibers, R206L+T204E attenuated the magnitude of the length-mediated recruitment of new cross-bridges (≈28%), suggesting that the Frank-Starling mechanism was impaired.

***Conclusions*—**Our findings are the first (to our knowledge) to demonstrate that the functional effects of a DCM-linked TnT mutation are not only modulated by MHC isoforms, but also by the pathology-associated post-translational modifications of TnT.
(*J Am Heart Assoc*. 2016;5:e002777 doi: 10.1161/JAHA.115.002777)

Key Words: dilated cardiomyopathy • myosin heavy chain • post-translational modification • protein kinase C • troponin T

Dilated cardiomyopathy (DCM) is a pathological condition of the heart characterized by systolic dysfunction and ventricular dilation.[1,2] Causes of DCM include heritable mutations found in sarcomeric proteins, such as cardiac troponin T (TnT).[1,3,4] It is still unclear how such DCM-linked mutations in TnT influence the molecular mechanisms that lead to contractile dysfunction and eventually heart failure. Our study focused on two reasons that limit our understanding: First, the functional effects of DCM mutations have mostly been studied using transgenic mice that express α-myosin heavy chain (MHC), whereas the human heart predominantly expresses β-MHC. Because α- and β-MHC differentially influence the functional effects of TnT, as demonstrated by an ever-increasing number of studies,[5–10] it is imperative that studies are carried out against the relevant MHC background to meaningfully evaluate the functional implications of DCM-linked mutations in human TnT. Second, complications arising from DCM-linked pathology may not only be dependent on the primary dysfunction caused by the mutation, but also on changes in post-translational modifications (PTMs).[11,12] In this regard, we chose to focus on one PTM and its link to DCM-mediated contractile dysfunction and pathogenesis. Specifically, we chose the protein kinase C (PKC)-mediated phosphorylation of TnT because PKC isoforms (α, βII, ε, δ, and ζ) that phosphorylate TnT (residues T195, S199, T204, S276, and T285 in rat TnT)[13–15] are upregulated in failing human hearts.[16,17] Moreover, several studies have demonstrated that in vitro PKC-mediated phosphorylation of TnT results in attenuated contractile function (for review, see Streng et al.[18]), as observed in failing hearts.

From the Department of Integrative Physiology and Neuroscience Washington State University, Pullman, WA.

Correspondence to: Murali Chandra, PhD, Department of Integrative Physiology and Neuroscience, 205 Veterinary Biomedical Research Building, Washington State University, Pullman, WA 99164-7620. E-mail: murali@vetmed.wsu.edu

Received October 9, 2015; accepted February 8, 2016.

DCM-related mutations in general have been shown to cause mild-to-moderate decrease in myofilament Ca^{2+} sensitivity and, in some cases, maximal tension.[3,19] Therefore, it is hard to understand how such mild effects can result in a variable pathogenesis that ranges from an asymptomatic phenotype to sudden cardiac death.[1,4] In some cases, the clinical expression of the disease is age dependent,[4] similar to pathology-linked cellular mechanisms, such as regulation of various PKC isoforms.[17,20] This leads us to an interesting point raised by Towbin and Solaro,[21] who alluded to the possibility that the functional effects of DCM-linked mutations could be exacerbated by PKC-mediated phosphorylation of adjacent residues. Therefore, a novel aspect of our study was to investigate whether PKC-mediated phosphorylation of TnT modulated the functional effects of R205L, a DCM mutation in human TnT linked to sudden cardiac death.[1] To emulate the effects of PKC-mediated phosphorylation of TnT, we used a PKC phosphomimic, where glutamate replaces threonine 204 in the rat TnT (T204E). Previously, threonine 204 was identified as the functionally critical residue for the effects of PKC-mediated phosphorylation of TnT.[14] Interestingly, the PKC phosphomimic, T204E, and the DCM mutation, R206L (rat analog of human R205L), are both located in the H1-helix of TnT (residues 203–221 in rat TnT), a domain of both structural[22,23] and functional relevance.[6,24] The structural relevance of the H1-helix of TnT is highlighted by its pivotal position between the core and tail domain of Tn[22] and also its direct interaction with tropomyosin.[23] The functional relevance of the H1-helix of TnT is demonstrated during thin-filament activation; Ca^{2+}-mediated structural changes in the troponin (Tn) core are transmitted to the Tn tail domain and Tm by the H1-helix of TnT. Moreover, the H1-helix of TnT modulates Ca^{2+} binding to TnC[24,25] and cross-bridge (XB) cycling kinetics.[5,6,26] Inferences based on the interplay between H1-helix of TnT- and XB-mediated effects on the thin filament[5,6,24] and the proximity of T204E and R206L to each other led to our hypothesis: The modulatory influence of T204E on R206L-mediated effects are differently affected by α- and β-MHC isoforms.

We tested our hypothesis by generating the following recombinant rat TnT variants: wild-type (WT); R206L; T204E (previously published[6]); and R206L+T204E. Recombinant TnT variants were reconstituted into detergent-skinned cardiac papillary muscle fibers taken from normal rats (expressing α-MHC) and propylthiouracil (PTU)-treated rats (expressing β-MHC). Steady-state and dynamic measurements were made on these reconstituted fibers. Our findings provide a molecular basis for the relatively severe effects of R206L against the α-MHC background and a subtle cardiac contractile phenotype against the β-MHC background. Moreover, our study may implicate the involvement of PTMs as additional factors that exacerbate the DCM-linked contractile dysfunction of the heart in some individuals.

Materials and Methods

Ethical Approval and Animal Treatment Protocols

Animals used in this study were treated in accord with the established guidelines approved by the Washington State University Institutional Animal Care and Use Committee. We used ≈4-month-old male Sprague-Dawley rats, which were divided into 2 groups: The first group consisted of normal rats (n=8) that expressed predominantly α-MHC in their ventricles, whereas the second group consisted of PTU-treated rats (n=6) that expressed β-MHC. PTU treatment lasted ≈4.5 weeks; rats were on water containing 0.2 g of PTU/liter (L) and a solid diet containing 0.15% PTU (Harlan Laboratories, Madison, WI). Rats were handled gently to minimize pain in strict compliance with the guidelines of the National Academy of Sciences Guide for the Care and Use of Laboratory animals.

Preparation of Detergent-Skinned Cardiac Muscle Fiber Bundles

We prepared detergent-skinned cardiac papillary muscle fibers, as previously described.[6] In brief, rats were deeply anaesthetized by an inhalation overdose of isoflourane. Hearts from the anesthetized rats were rapidly excised and placed into an ice-cold high relaxing (HR) solution containing (in mmol/L): 20 BDM; 50 BES; 20 EGTA; 6.29 $MgCl_2$; 6.09 Na_2ATP; 30.83 potassium propionate; 10 NaN_3; 1.0 DTT; and 4 benzamidine-HCl; and a cocktail of protease inhibitors (in μmol/L): 5 bestatin; 2 E-64; 10 leupeptin; 1 pepstatin; and 200 PMSF. KOH was used to set the pH of the HR solution to 7.0. Muscle bundles excised from the left ventricles were further dissected into smaller fibers of dimensions, ≈2 mm in length and ≈0.15 mm in width, in the HR solution. Muscle fibers were demembranated by overnight detergent skinning at 4°C in HR solution that contained 1% Triton X-100.

Preparation of Left Ventricular Protein Samples

We prepared left ventricular protein samples, as previously described.[6,9] In brief, rat hearts were flash frozen in liquid nitrogen and thoroughly pulverized using a pestle and mortar. Pulverized tissue was then resuspended in a protein extraction buffer (10 μL/mg of tissue) that contained: 2.5% SDS; 10% glycerol; 50 mmol/L Tris base (pH 6.8 at 4°C); 1 mmol/L of DTT, 1 mmol/L of PMSF; 4 mmol/L of benzamidine-HCl; and protease inhibitors (E-64, leupeptin, and bestatin). A "Tissue Tearor" (model 985370-395; BioSpec Products, Inc., Bartlesville, OK) was used to further homogenize the resuspended tissue, followed by sonication in a water bath at 4°C, and finally centrifuged at 6708*g*. Supernatant from the above-prepared protein samples were run on a large 4% SDS gel and

stained with Bio-Safe Coomassie blue G-250 (Bio-Rad Laboratories, Inc., Hercules, CA) to compare levels of MHC isoforms between normal and PTU-treated rat hearts.

Expression and Purification of Recombinant Rat Cardiac Tn Subunits

Recombinant *c-myc* tagged WT rat TnT, *c-myc* tagged R206L mutant TnT (R206L), *c-myc* tagged R206L+T204E mutant TnT (R206L+T204E), rat cardiac troponin I (TnI), and rat cardiac troponin C (TnC) were all cloned into a pSBETa vector (GenScript USA, Inc., Piscataway Township, NJ) and expressed in BL21*DE3 cells (Novagen, Madison, WI).[27] BL21*DE3 cells were transformed with the respective TnT-variant plasmid (WT, R206L, and R206L+T204E), cultured overnight, spun down, and sonicated in the extraction buffer, which contained 50 mmol/L of Tris base (pH 8.0 at 4°C), 6 mol/L of urea, 5 mmol/L of EDTA, and a cocktail of protease inhibitors, such as 0.2 mmol/L of PMSF, 5 mmol/L of benzamidine-HCl, 10 μmol/L of leupeptin, 1 μmol/L of pepstatin, 5 μmol/L of bestatin, 2 μmol/L of E-64, and 1 mmol/L of DTT. The sonicated preparation was centrifuged to pellet out the insoluble cellular particulates, and the supernatant was used for the ammonium sulfate fractionation procedure. The pellet from 70% ammonium sulfate fractionation was dissolved in 50 mmol/L of Tris base (pH 8.0 at 4°C), 6 mol/L of urea, 0.5 mmol/L of EDTA, 0.4 mmol/L of PMSF, 5 mmol/L of benzamidine-HCl, 0.01% NaN_3, and 1 mmol/L of DTT and then purified by ion-exchange chromatography on a DEAE-fast sepharose column (GE Healthcare Biosciences, Pittsburgh, PA). TnT variants were eluted with a 0- to 1-mol/L NaCl gradient. TnC and TnI were purified as described previously.[28,29] All eluted protein fractions were run on a 12.5% SDS gel to determine their purity. Pure protein fractions were pooled and dialyzed extensively against deionized water containing 15 mmol/L of β-mercaptoethanol, lyophilized, and stored at −80°C.

Reconstitution of Recombinant Rat Cardiac Tn Into Demembranated Rat Cardiac Muscle Fibers

We reconstituted recombinant Tn into demembranated rat cardiac muscle fibers, as described previously.[27] In brief, we used an extraction buffer containing TnT (WT or R206L or R206L+T204E; 0.9 mg/mL, w/v) and TnI (1.0 mg/mL, w/v) to replace the endogenous Tn complex by the law of mass action. To prepare the extraction buffer, we dissolved both proteins in buffer 1, which contained 50 mmol/L of Tris-HCl (pH 8.0 at 4°C), 6 mol/L of urea, 1.0 mol/L of KCl, 1 mmol/L of DTT, and a cocktail of protease inhibitors. Excess urea and salt were removed by successive dialysis against the following buffers: 50 mmol/L of Tris-HCl (pH 8.0 at 4°C), 4 mol/L of urea, 0.7 mol/L of KCl, 0.2 mmol/L of PMSF, 2 mmol/L of benzamidine-HCl, 1 mmol/L of DTT, and 0.01% NaN_3 (buffer 2), followed by 50 mmol/L of Tris-HCl (pH 8.0 at 4°C), 2 mol/L of urea, 0.5 mol/L of KCl, 0.2 mmol/L of PMSF, 2 mmol/L of benzamidine-HCl, 1 mmol/L of DTT, and 0.01% NaN_3 (buffer 3), and finally dialyzed against an extraction buffer containing 50 mmol/L of BES (pH 7.0 at 20°C), 0.2 mol/L of KCl, 10 mmol/L of BDM, 6.27 mmol/L of $MgCl_2$, 5 mmol/L of EGTA, 0.2 mmol/L of PMSF, 2 mmol/L of benzamidine-HCl, 1 mmol/L of DTT, and 0.01% NaN_3 (buffer 4). After the dialysis in buffer 4, a cocktail of protease inhibitors along with 6.13 mmol/L of $MgATP^{2-}$ was added to the dialysate. The dialysate was then centrifuged at 805*g* for 15 minutes to remove any undissolved proteins. The supernatant containing TnT and TnI was used to treat the demembranated fibers for ≈3 hours at room temperature (20°C), with constant stirring. This was followed by washing the treated muscle fibers twice using buffer 4 for 10 minutes at room temperature and incubating them with TnC (3.0 mg/mL, w/v) at 4°C to complete the reconstitution procedure. We used the following nomenclature to denote the various groups of fibers based on the MHC isoform background and the TnT variant present in exogenous Tn complex: Detergent-skinned α-MHC and β-MHC fibers reconstituted with *c-myc* TnT+TnI+TnC are referred to as "α-MHC+WT" and "β-MHC+WT," respectively. Similarly, α-MHC and β-MHC fibers reconstituted with *c-myc* R206L+TnI+TnC are referred to as "α-MHC+R206L" and "β-MHC+R206L," respectively. Finally, α-MHC and β-MHC fibers reconstituted with *c-myc* R206L+T204E+TnI+TnC are referred to as "α-MHC+R206L+T204E" and "β-MHC+R206L+T204E," respectively. α-MHC+WT and β-MHC+WT were used as controls in the respective groups.

Western Blot Analysis of the Reconstituted Fibers

The extent of removal of the endogenous Tn by the exogenous Tn complex was assessed by the differential migration pattern of *c-myc*-tagged TnT, when compared to endogenous TnT.[30] Muscle fibers were first solubilized by incubating in a muscle protein extraction buffer (≈5 μL per fiber) for an hour at 4°C. The extraction buffer was composed of 2.5% SDS, 50 mmol/L of Tris base (pH 6.8 at 4°C), 10% glycerol, 1 mol/L of DTT, and a cocktail of protease inhibitors. Fibers were further solubilized by sonication in a water bath for 20 minutes at 4°C. To the sonicated preparation, an equal amount of protein loading dye (composed of 125 mmol/L of Tris-HCl [pH 6.8], 20% glycerol, 2% SDS, 0.01% bromophenol blue, and 50 mmol/L of β-mercaptoethanol) was added. Proteins were separated on an 8% SDS gel and transferred onto a PVDF membrane for Western blot analysis using a Trans-Blot Turbo Transfer System (Bio-Rad Laboratories, Inc., Hercules, CA). Extent of incorporation of *c-myc* TnT (WT or R206L or R206L+T204E) was assessed using a monoclonal anti-TnT primary antibody (clone JLT-12; Sigma-

Aldrich, St Louis, MO), and a HRP-labeled antimouse secondary antibody (Amersham Biosciences, Pittsburgh, PA). Densitometric analysis of Western blots was done using ImageJ software (from NIH at: http://rsbweb.nih.gov/ij/). Cumulative optical band intensities of endogenous TnT and reconstituted *c-myc*-tagged TnT variants were taken as the total amount of TnT in a single lane. Optical band intensity of the exogenously added TnT variant was divided by the optical band intensity of the total amount of TnT to estimate the extent of the exogenous TnT incorporation.

Steady-State Isometric Tension and ATPase Activity

Isometric steady-state tension and ATPase activity were estimated as described previously.[27,31–33] In brief, aluminum clips were used to hang the fiber between a motor arm (322C; Aurora Scientific, Inc., Aurora, Ontario, Canada) and a force transducer (AE 801; Sensor One Technologies Corp., Sausalito, CA). The sarcomere length (SL) of the muscle fiber was set to 2.3 μm using a He-Ne laser diffraction pattern, as described previously.[27] After 2 cycles of maximal activation and relaxation, if deemed necessary, the SL was readjusted. The muscle fiber was then activated by lowering it in a constantly stirred chamber containing Ca^{2+} solutions. The concentration of the Ca^{2+} solutions ranged from pCa 4.3 to 9.0 (pCa=−log of $[Ca^{2+}]_{free}$), and their compositions were calculated using methods described previously.[34] The maximal Ca^{2+} activation solution (pCa 4.3) contained (in mmol/L): 31 potassium propionate; 5.95 Na_2ATP; 6.61 $MgCl_2$; 10 EGTA; 10.11 $CaCl_2$; 50 BES; 5 NaN_3; and 10 phosphoenol pyruvate (PEP). The relaxing solution (pCa 9.0) contained (in mmol/L): 51.14 potassium propionate; 5.83 Na_2ATP; 6.87 $MgCl_2$; 10 EGTA; 0.024 $CaCl_2$; 50 BES; 5 NaN_3; and 10 PEP. Activation and relaxing solutions also contained 0.5 mg/mL of pyruvate kinase (≈350 U/mg; 151999; MP Biomedicals, Santa Ana, CA), 0.05 mg/mL of lactate dehydrogenase (≈700–1200 U/mg; L1254; Sigma-Aldrich), 20 μmol/L of diadenosine pentaphosphate, 10 μmol/L of oligomycin, and a cocktail of protease inhibitors. The ionic strength was 180 mmol/L, and the pH was adjusted to 7.0. Ca^{2+}-activated steady-state tensions were recorded on a computer.

Ca^{2+}-activated steady-state ATPase activity was measured according to a protocol described previously.[27,31,32] In brief, near-UV light was projected through the muscle chamber, split (50:50) using a beam splitter, and detected at 400 nm (insensitive to changes in NADH) and 340 nm (sensitive to changes in NADH). ATPase activity was measured using the following enzyme-coupled assay: ATP regeneration from ADP was coupled to the breakdown of PEP to ATP and pyruvate catalyzed by pyruvate kinase, which was, in turn, coupled to the synthesis of lactate catalyzed by lactate dehydrogenase. Breakdown of NADH was proportional to the amount of ATP utilized by cycling XBs and was measured by changes in UV absorbance at 340 nm. The signal for NADH breakdown was calibrated by multiple injections of 250 pmol of ADP. All measurements were made at 20°C.

Muscle Fiber Mechano-Dynamics

Ca^{2+}-activated muscle fibers were subjected to step-like length perturbations in the order of ±0.5%, ±1.0%, ±1.5%, and ±2.0% of the initial muscle length (ML), as described previously.[35] The resultant force responses were used to fit a nonlinear recruitment distortion (NLRD) model in order to estimate model parameters such as: the magnitude of the instantaneous muscle fiber stiffness attributed to a sudden change in ML (E_D); the rate at which the strain of distorted XBs rapidly dissipates after a change in ML (c); the rate at which new force-generating XBs are recruited because of a change in ML (b); and the magnitude of an increase in muscle fiber stiffness attributed to the ML-mediated recruitment of new XBs (E_R).

The following describes the various model parameters and their physiological relevance:

1 Phase 1: In response to a sudden increase in ML (Figure 1A), the instantaneous increase in force, from F_{ss} to F_1 (Figure 1B), denotes phase 1. Two reasons underlie the instantaneous increase in force: (1) the rapid distortion of the elastic elements in the strongly bound XBs; and (2) the change in ML (ΔL) is much faster than the recruitment of new XBs. Therefore, E_D, which is estimated as the slope of the relationship between ($\Delta F=F_1-F_{ss}$) and ΔL, is an approximation of the number of strongly bound XBs.[35] Thus, an augmentation of E_D is indicative of an increase in the number of strongly bound XBs, whereas an attenuation of E_D is indicative of a decrease in the number of strongly bound XBs.

2 Phase 2: This refers to the rapid decline in force to a minimum (nadir; Figure 1B), as the fiber is held at the new ML (Figure 1A). As suddenly stretched XBs detach, force declines rapidly. Previous studies have indicated that the dynamic rate at which the force decays (c) is an index of XB detachment rate.[27,35,36]

3 Phase 3: This refers to the steady rise in force (Figure 1B), after the change in ML (Figure 1A). The change in ML leads to recruitment of additional XBs. Force rises at a dynamic rate (b) to a new steady-state level (Figure 1B).

4 F_{nss}: The steady rise in force (Phase 3) eventually levels off to a new steady state (F_{nss}). The magnitude of force increase, from F_{ss} to F_{nss}, is proportional to the recruitment of additional force-bearing XBs. Therefore, E_R, which is estimated as the slope of the relationship between ($F_{nss}-F_{ss}$) and ΔL, is the magnitude of the ML-mediated recruitment of new force-bearing XBs.

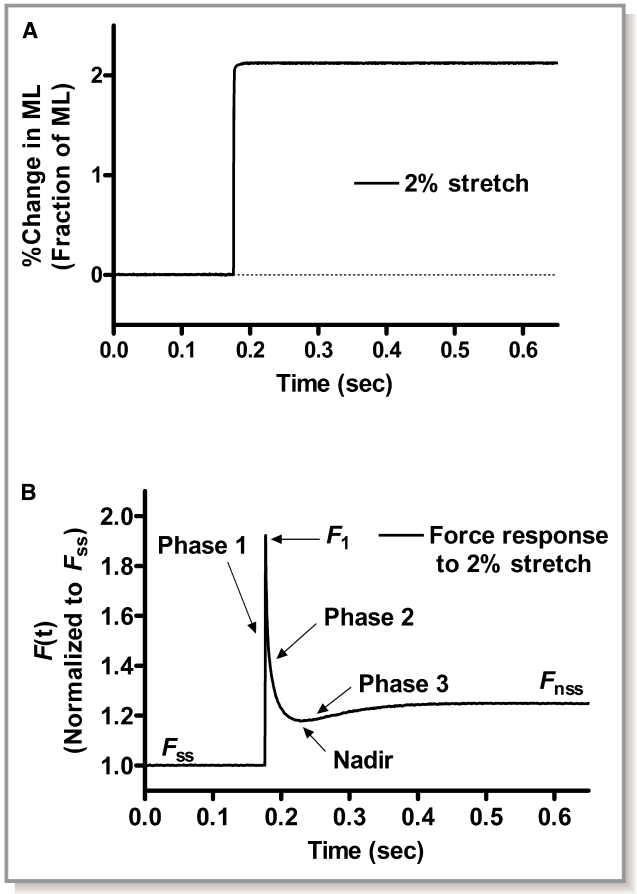

Figure 1. Representative force trace in response to a large amplitude (+2%) step-like length perturbation of a maximally Ca^{2+}-activated rat cardiac muscle fiber. A family of force responses to step-like length perturbations of various magnitudes were fit using the nonlinear recruitment distortion (NLRD) model to estimate several parameters, as described earlier.[35] A, Representative length trace of a maximally activated muscle fiber subjected to a 2% step-like increase in the initial muscle length (ML). B, The corresponding force response of an α-MHC+WT fiber normalized to isometric steady-state force (F_{ss}), just before the stretch. The different phases from which the respective NLRD parameters were estimated are highlighted; please refer to the Materials and Methods for details on the NLRD parameters and their physiological relevance. α-MHC, alpha myosin heavy chain; WT, wild type.

Measurement of Rate of Tension Redevelopment (k_{tr})

We estimated k_{tr} using a modified version of the protocol[32,37] originally described by Brenner and Eisenberg.[38] A maximally Ca^{2+}-activated fiber, on reaching isometric steady-state tension, was slackened by 10% of the initial ML using a high-speed length-control device (322C; Aurora Scientific, Inc., Aurora, Ontario, Canada). After a brief shortening period of 25 ms, the motor arm was commanded to stretch the fiber by 10% of the original ML to ensure detachment of any residual XBs. k_{tr} was determined by fitting the following monoexponential equation to the force redevelopment.

$$F(t) = (F_{ss} - F_{res})\,(1 - e^{-k_{tr}t}) + F_{res}$$

where $F(t)$ is the force at time t, F_{ss} is the steady-state isometric force, and F_{res} is the residual force from which the redevelopment of force occurs.

Statistical Analysis

Two-way ANOVA was used to analyze the steady-state and dynamic parameters because there were 2 experimental factors: MHC isoform (α-MHC and β-MHC) and TnT variants (WT, R206L, T204E, and R206L+T204E). A significant interaction effect suggested that the functional effects of TnT variants were differently affected by α- and β-MHC isoforms. When the interaction effect was not significant, we interpreted the main effects attributed to the TnT variants. To test the functional impact of the TnT variants on various contractile parameters, post-hoc multiple comparisons were made using Fisher's uncorrected least significant differences (LSD) method. Data from an earlier study on T204E-mediated effects[6] was included in the 2-way ANOVA because we wanted to isolate the individual effects of T204E and R206L, while investigating the functional effects of R206L+T204E. To elaborate, when post-hoc multiple comparisons revealed that R206L+T204E was significantly different from WT, then we compared whether R206L+T204E was also significantly different from T204E. To ensure that valid comparisons can be made with the previously published T204E data[6] and our current data, we maintained identical experimental conditions (treatment of animals, cardiac tissue extraction procedures, reconstitution procedures, the same batch of solutions, and other experimental conditions) in both studies. Because comparable amounts of exogenous TnT variants were incorporated into the detergent-skinned fibers in both studies, it also confirmed that the experimental conditions were similar. pCa_{50} (−log of $[Ca^{2+}]_{free}$ required for half-maximal activation) and the Hill coefficient (n_H) were estimated by fitting the Hill equation to the normalized pCa-tension data. Values are reported as mean±SEM. The criterion for statistical significance was set at $P<0.05$.

Results

PTU Treatment Causes the MHC Isoform to Shift From α- to β-MHC in Rat Hearts

We and others have demonstrated that PTU treatment causes the MHC isoform to shift completely from α- to β-MHC, without having any significant impact on the level of expression of other myofilament proteins.[6,39–41] Figure 2A demonstrates that PTU treatment leads to 100% β-MHC in PTU-treated rat hearts.

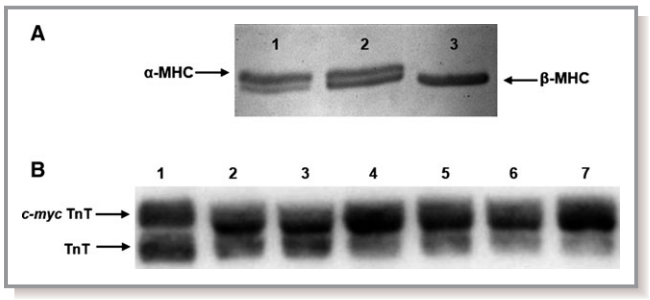

Figure 2. Gel analysis. A, SDS-PAGE to illustrate the shift in MHC isoform. Lanes 1 and 3 show heart samples prepared from normal and PTU-treated rats, respectively. Lane 2 shows an intermediate mix of protein samples prepared from normal and PTU-treated rat hearts. PTU-treated rat hearts demonstrate a complete shift from α- to β-MHC. B, Western blot analysis of reconstituted fibers. Lane 1 shows purified recombinant TnT and *c-myc* TnT. Reconstituted fiber samples are in the following lanes: α-MHC+WT (lane 2); α-MHC+R206L (lane 3); α-MHC+R206L+T204E (lane 4); β-MHC+WT (lane 5); β-MHC+R206L (lane 6); and β-MHC+R206L+T204E (lane 7). MHC, myosin heavy chain; PTU, propylthiouracil; TnT, troponin T; WT, wild type.

Western Blot Analysis of Reconstituted α- and β-MHC Fibers

Western blot analysis was used to quantify the extent of incorporation of the exogenous Tn complex in the reconstituted fibers, as described in Materials and Methods. The following values from 3 gels are reported as mean±SEM. The extent of incorporation in α-MHC fibers was as follows: 75±2% in WT (lane 2 of Figure 2B); 74±2% in R206L (lane 3 of Figure 2B); and 72±4% in R206L+T204E (lane 4 of Figure 2B). In β-MHC fibers, the extent of incorporation was as follows: 72±3% in WT (lane 5 of Figure 2B); 71±6% in R206L (lane 6 of Figure 2B); and 66±8% in R206L+T204E (lane 7 of Figure 2B).

Effects of α- and β-MHC Isoforms on the R206L- and R206L+T204E-Mediated Impact on Ca^{2+}-Activated Maximal Tension and ATPase Activity

The cardiac myofilament is a tightly coupled allosteric/cooperative system[42]; therefore, a significant interplay is expected between the TnT- and MHC-mediated effects on the thin filament.[6,9] Therefore, we investigated whether the R206L- and R206L+T204E-mediated effects on the thin filament are modulated differently by α- and β-MHC isoforms, by measuring Ca^{2+}-activated maximal tension and ATPase activity, as described in Materials and Methods. Two-way ANOVA of Ca^{2+}-activated maximal tension showed a significant interaction effect ($P<0.001$) between the 2 factors (the MHC isoforms and the TnT variants). This demonstrates that α- and β-MHC isoforms have different impact on how the TnT variants (R206L, T204E, or R206L+T204E) alter Ca^{2+}-activated maximal tension (Figure 3A). Subsequent post-hoc tests (multiple pair-wise comparisons) were carried out to identify the factors that were responsible for the interaction effect. In α-MHC fibers, R206L attenuated Ca^{2+}-activated maximal tension by ≈32% ($P<0.001$), while T204E and R206L+T204E attenuated tension by ≈63% ($P<0.001$) and ≈64% ($P<0.001$), respectively (Figure 3A). In agreement with our observations, previous studies have demonstrated that R206L[19] and the PKC phosphomimic of TnT (T204E)[14] attenuate tension. What is interesting to note is that although R206L attenuates tension by itself in α-MHC fibers, it has no additive effect on the influence of T204E on tension in α-MHC+R206L+T204E fibers. On the other hand, in β-MHC fibers, R206L did not alter Ca^{2+}-activated maximal tension (Figure 3A), whereas T204E and R206L+T204E attenuated tension by ≈33% ($P<0.001$) and ≈40% ($P<0.001$), respectively (Figure 3A). These observations reveal 3 interesting effects of β-MHC: (1) It abolished the attenuating effect of R206L on tension; (2) it minimized the attenuating effects of T204E and R206L+T204E on tension; and (3) it facilitated R206L+T204E to exacerbate the T204E-mediated attenuation in tension by ≈11% ($P<0.05$; Figure 3A). This suggests that the interplay between β-MHC-, R206L-, and T204E-mediated effects on the thin filament exacerbated the attenuation in tension.

The estimates of ATPase activity (in $pmol \cdot mm^{-3} \cdot s^{-1}$) in various groups are as follows: 205±6 for α-MHC+WT; 113±6 for α-MHC+R206L; 67±5 for α-MHC+T204E; 61±4 for α-MHC+R206L+T204E; 109±4 for β-MHC+WT; 79±2 for β-MHC+R206L; 78±3 for β-MHC+T204E; and 52±3 for β-MHC+R206L+T204E. Two-way ANOVA of Ca^{2+}-activated maximal ATPase activity demonstrated a significant interaction effect ($P<0.001$), indicating that α- and β-MHC had differential impact on how the TnT variants altered ATPase activity. Subsequent post-hoc tests revealed the following: In α-MHC fibers, R206L, T204E, and R206L+T204E decreased maximal ATPase activity by ≈45% ($P<0.001$), ≈67% ($P<0.001$), and ≈70% ($P<0.001$), respectively. These observations are in agreement with previous studies, which demonstrate that both R206L[19] and T204E[14] attenuate maximal ATPase activity. As observed in tension estimates, although R206L attenuates ATPase rate by itself in α-MHC fibers, it has no additive influence on the T204E-mediated effect on ATPase activity of α-MHC+R206L+T204E fibers. However, in β-MHC fibers, R206L, T204E, and R206L+T204E decreased maximal ATPase activity by ≈28% ($P<0.001$), ≈28% ($P<0.001$), and ≈52% ($P<0.001$), respectively. This shows that β-MHC not only minimized the attenuating effects of the TnT variants on ATPase activity, but also facilitated R206L+T204E to exacerbate the T204E-mediated attenuation

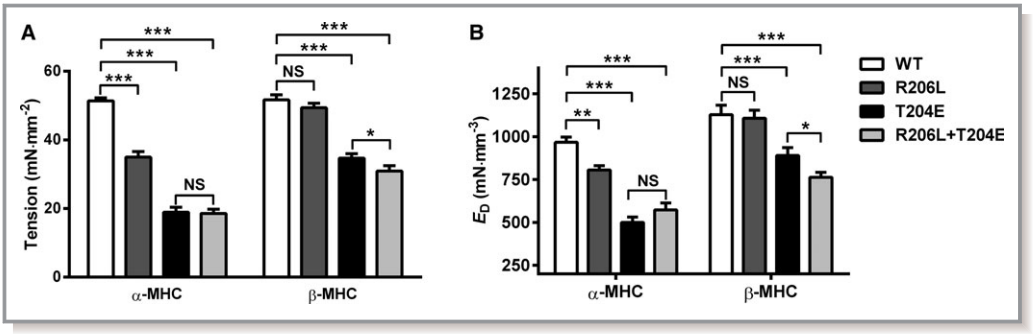

Figure 3. Effects of α- and β-MHC isoforms on the R206L- and R206L+T204E-mediated impact on Ca^{2+}-activated maximal tension and E_D. Both parameters were estimated as described in the Materials and Methods. Bar graphs showing the differential impacts of the TnT variants on (A) Ca^{2+}-activated maximal tension (pCa 4.3) and (B) E_D in α- and β-MHC fibers. Data were analyzed using 2-way ANOVA, and subsequent post-hoc multiple pair-wise comparisons were made using Fisher's LSD method. Asterisks indicate a statistically significant result when compared to respective control fibers (*P<0.05; **P<0.01; ***P<0.001; NS). Fibers from 3 normal and 3 PTU-treated rat hearts were used for investigating each of the TnT variants in this study. For tension, n=16 for α-MHC+WT; 15 for α-MHC+R206L; 15 for α-MHC+T204E; 19 for α-MHC+R206L+T204E; 14 for β-MHC+WT; 15 for β-MHC+R206L; 19 for β-MHC+T204E; and 19 for β-MHC+R206L+T204E. For E_D, n=16 for α-MHC+WT, 15 for α-MHC+R206L, 15 for α-MHC+T204E, 15 for α-MHC+R206L+T204E, 14 for β-MHC+WT, 15 for β-MHC+R206L, 19 for β-MHC+T204E, and 16 for β-MHC+R206L+T204E. Values are reported as mean±SEM. MHC indicates myosin heavy chain; n, number of fibers in each group; LSD, least significant difference; NS, not significant; PTU, propylthiouracil; TnT, troponin T; WT, wild type.

in ATPase rate by ≈33% (P<0.001). Thus, our observations suggest an interplay between the β-MHC-, R206L-, and T204E-mediated effects on the thin filament, as observed in the tension experiments. An exception to this is that attenuation of ATPase activity was disproportionate to tension in α-MHC+R206L and β-MHC+R206L fibers, suggesting that R206L slows XB detachment kinetics.

Effects of α- and β-MHC Isoforms on the R206L- and R206L+T204E-Mediated Impact on E_D

We estimated E_D to determine whether the number of force-bearing XBs were altered by the interplay between the MHC isoform- and TnT variant-mediated effects on the thin filaments. As we have demonstrated previously, E_D is an approximation of the number of force-bearing XBs,[35,37] and it was estimated as described in Materials and Methods. Two-way ANOVA of E_D revealed that the interaction effect was significant (P<0.05), indicating that α- and β-MHC had differential impact on how TnT variants altered E_D. Post-hoc multiple pair-wise comparisons were carried out to determine the factors responsible for the interaction effect. In α-MHC fibers, R206L attenuated E_D by ≈17% (P<0.01), while T204E and R206L+T204E attenuated E_D by ≈48% (P<0.001) and ≈41% (P<0.001), respectively (Figure 3B). In β-MHC fibers, R206L did not alter E_D (Figure 3B), but T204E and R206L+T204E attenuated E_D by ≈21% (P<0.001) and ≈32% (P<0.001), respectively (Figure 3B). Thus, just as we observed in tension experiments, β-MHC has 3 interesting effects: (1) It abolished the attenuating effects of R206L on the number of force-bearing XBs; (2) it minimized the attenuating effect of T204E and R206L+T204E on the number of force-bearing XBs (Figure 3B); and (3) it facilitated R206L+T204E to exacerbate the T204E-mediated attenuation in E_D by ≈14% (P<0.05; Figure 3B). These observations provide substantiating experimental evidence for the differential effects of α- and β-MHC on the R206L- and R206L+T204E-mediated effects on Ca^{2+}-activated maximal tension.

Effects of α- and β-MHC Isoforms on the R206L- and R206L+T204E-Mediated Impact on Myofilament Ca^{2+} Sensitivity

To investigate the impact of the interplay between the MHC isoform- and TnT variant-mediated effects on myofilament Ca^{2+} sensitivity, we estimated pCa_{50} by fitting the Hill equation to the normalized pCa-tension data (Figure 4A and 4B). Two-way ANOVA revealed no significant interaction effect, indicating that α- and β-MHC did not have differential impact on how the TnT variants altered pCa_{50} (Figure 4C). The main effect of TnT variants on pCa_{50} was significant (P<0.001); therefore, in order to determine which of the TnT variants caused this main effect, post-hoc multiple pair-wise comparisons were carried out. In α-MHC fibers, R206L, T204E, and R206L+T204E significantly decreased pCa_{50} by ≈0.08 pCa units (P<0.001), ≈0.31 pCa units (P<0.001), and ≈0.33 pCa units (P<0.001), respectively (Figure 4C). In β-

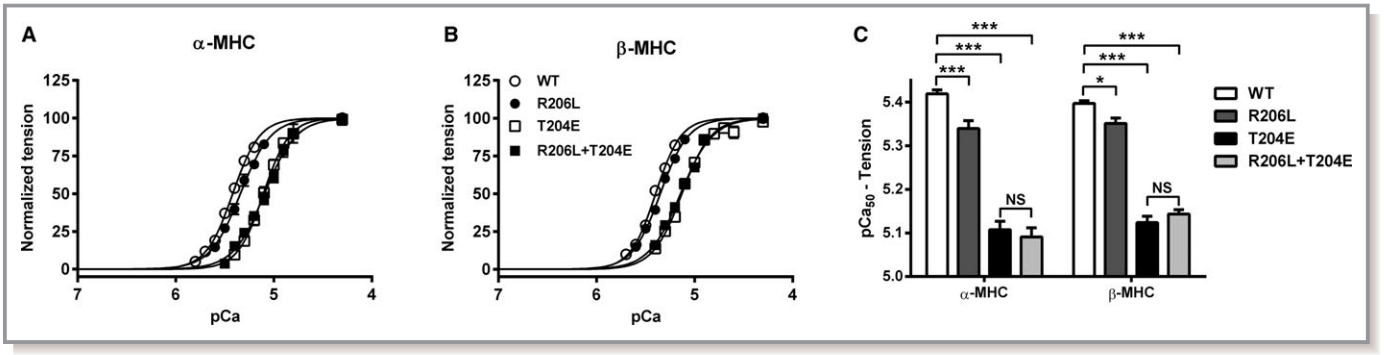

Figure 4. Effects of α- and β-MHC isoforms on the R206L- and R206L+T204E-mediated impact on pCa_{50}. pCa-tension relationships were estimated by plotting normalized tension values against a range of pCa (4.3–9.0). The Hill equation was fit to the pCa-tension relationships to estimate pCa_{50} and n_H, as described in the Materials and Methods. pCa-tension relationship of the averaged values of reconstituted (A) α-MHC and (B) β-MHC fibers. C, Bar graph showing the differential impacts of TnT variants on pCa_{50}. Data were analyzed using 2-way ANOVA, and subsequent post-hoc multiple pair-wise comparisons were made using Fisher's LSD method. Asterisks indicate a statistically significant result when compared to respective control fibers (*P<0.05; ***P<0.001; NS). Fibers from 3 normal and 3 PTU-treated rat hearts were used for investigating each of the TnT variants in this study. n=16 for α-MHC+WT, 15 for α-MHC+R206L, 15 for α-MHC+T204E, 17 for α-MHC+R206L+T204E, 14 for β-MHC+WT, 15 for β-MHC+R206L, 19 for β-MHC+T204E and 16 for β-MHC+R206L+T204E. Values are reported as mean±SEM. MHC indicates myosin heavy chain; n, number of fibers in each group; LSD, least significant difference; NS, not significant; PTU, propylthiouracil; TnT, troponin T; WT, wild type.

MHC fibers, R206L, T204E, and R206L+T204E significantly decreased pCa_{50} by ≈0.05 pCa units (P<0.05), ≈0.27 pCa units (P<0.001), and ≈0.25 pCa units (P<0.001), respectively (Figure 4C). Thus, regardless of the type of MHC isoform present, myofilament Ca^{2+} sensitivity was modestly attenuated by R206L and greatly attenuated by T204E. It is interesting to note that, except myofilament Ca^{2+} sensitivity, all other contractile parameters that were affected by either R206L or T204E were further modulated differently by α- and β-MHC isoforms. These observations suggest that the R206L- and T204E-mediated effects on myofilament Ca^{2+} sensitivity are acting independent of the molecular pathway that mediates interplay between the TnT- and MHC isoform-mediated effects on the thin filament.

Effects of α- and β-MHC Isoforms on the R206L- and R206L+T204E-Mediated Impact on Myofilament Cooperativity

To investigate whether an interplay between the MHC isoform- and TnT variant-mediated effects influenced myofilament cooperativity, we estimated n_H by fitting the Hill equation to the normalized pCa-tension data (Figure 4A and 4B). Two-way ANOVA of n_H revealed no significant interaction effect, but the main effect of the TnT variants on n_H was significant (P<0.01; Figure 5A). To determine which of the TnT variants caused this main effect, post-hoc multiple pair-wise comparisons were carried out. None of the TnT variants altered n_H in α-MHC fibers. In β-MHC fibers, n_H was also not altered by R206L or T204E alone; however, R206L+T204E decreased n_H by ≈19% (P<0.01; Figure 5A) in β-MHC fibers relative to WT and by ≈17% (P<0.01; Figure 5A) relative to T204E. Thus, these observations demonstrate that the cumulative effect of T204E and R206L on n_H is differentially altered by α- and β-MHC isoforms. Moreover, the interplay between β-MHC-, T204E-, and R206L-mediated effects on myofilament cooperativity could offer insights into how β-MHC+R206L+T204E exacerbated β-MHC+T204E-mediated attenuation in tension.

Effects of α- and β-MHC Isoforms on the R206L- and R206L+T204E-Mediated Impact on E_R

To determine whether the influences of the MHC isoform- and TnT variant-mediated effects on myofilament cooperativity also impacted length-dependent activation (LDA) of the cardiac myofilament, we estimated E_R. E_R is the magnitude of the ML-mediated recruitment of new XBs, and it was estimated as described in Materials and Methods. Two-way ANOVA revealed that the interaction effect was not significant, but the main effect of the TnT variants on E_R was significant (P<0.05). Post-hoc multiple pair-wise comparisons revealed that none of the TnT variants affected E_R in α-MHC fibers. In β-MHC fibers, E_R was also not affected by R206L or T204E alone; however, R206L+T204E decreased E_R by ≈28% (P<0.01; Figure 5B) relative to WT and by ≈21% (P<0.05; Figure 5B) relative to T204E. Thus, our E_R estimates demonstrate that LDA of the cardiac myofilament is blunted by the cumulative effects of β-MHC, R206L, and T204E on the thin filament. A similar trend in n_H (Figure 5A) suggests that the R206L+T204E-mediated effects on E_R are mediated by cooperative processes that modulate the interplay between the TnT- and MHC-mediated effects.

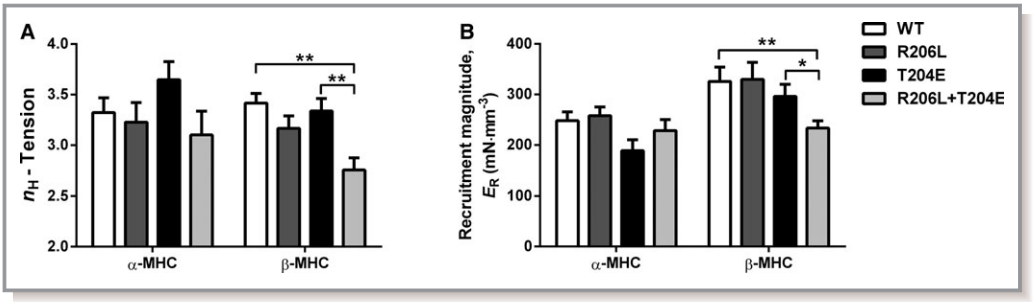

Figure 5. Effects of α- and β-MHC isoforms on the R206L- and R206L+T204E-mediated impact on n_H and E_R. Both parameters were estimated as described in the Materials and Methods. Bar graphs showing the differential impacts of TnT variants on (A) n_H and (B) E_R in α- and β-MHC fibers. Data were analyzed using 2-way ANOVA, and subsequent post-hoc multiple pair-wise comparisons were made using Fisher's LSD method. Asterisks indicate a statistically significant result when compared to respective control fibers (*P<0.05; **P<0.01). Fibers from 3 normal and 3 PTU-treated rat hearts were used for investigating each of the TnT variants in this study. For n_H, n=16 for α-MHC+WT, 15 for α-MHC+R206L, 15 for α-MHC+T204E, 17 for α-MHC+R206L+T204E, 14 for β-MHC+WT, 15 for β-MHC+R206L, 19 for β-MHC+T204E, and 16 for β-MHC+R206L+T204E. For E_R, n=16 for α-MHC+WT, 15 for α-MHC+R206L, 15 for α-MHC+T204E, 15 for α-MHC+R206L+T204E, 14 for β-MHC+WT, 15 for β-MHC+R206L, 19 for β-MHC+T204E, and 16 for β-MHC+R206L+T204E. Values are reported as mean±SEM. MHC indicates myosin heavy chain; n, number of fibers in each group; LSD, least significant difference; PTU, propylthiouracil; TnT, troponin T; WT, wild type.

Effects of α- and β-MHC Isoforms on the R206L- and R206L+T204E-Mediated Impact on XB Detachment Dynamics

We wanted to test whether the R206L- and T204E-mediated impact on the thin filament manifested as changes in XB cycling kinetics and whether such effects were differentially altered by α- and β-MHC isoforms. We determined XB detachment rate (g) by estimating tension cost and the rate of XB distortion dynamics (c). Tension cost was estimated as the slope of the ATPase-tension relationship, as described previously.[6,27] According to the 2-state model,[43] tension cost is correlated to g because the ratio of ATPase utilization rate ($fg/f+g$) to tension ($f/f+g$) is proportional to g, where f and g are XB attachment and detachment rates, respectively. Two-way ANOVA of tension cost revealed that the interaction effect was significant (P<0.01), demonstrating differential effects of α- and β-MHC isoforms on how TnT variants altered tension cost. Post-hoc multiple pair-wise comparisons revealed the following: in α-MHC fibers, R206L, T204E, and R206L+T204E decreased tension cost by ≈19% (P<0.001), ≈15% (P<0.001), and ≈16% (P<0.001), respectively (Figure 6A). In β-MHC fibers, T204E did not alter tension cost, but R206L and R206L+T204E decreased tension cost by ≈26% (P<0.01) and ≈24% (P<0.01), respectively (Figure 6A). There was a modest, but significant, decrease in g in α-MHC+T204E, but that effect is abolished in β-MHC+T204E. Another important observation from our tension cost measurements is that R206L slows g in both α- and β-MHC fibers, regardless of the influence of T204E.

To corroborate our conclusions from tension cost measurements, we measured XB distortion dynamics, c, as described in Materials and Methods. c represents the rate of detachment of strained XBs, and it was estimated as the rate at which a sudden stretch-induced increase in force decays to a minimum (Figure 1B).[35] Previously, it has been demonstrated that c is an index of g and there is a strong correlation between c and tension cost.[36] Two-way ANOVA of c revealed that the interaction effect between the MHC isoforms and TnT variants was significant (P<0.001). Post-hoc multiple pair-wise comparisons revealed information that is similar to what we observed in the tension cost measurements. In α-MHC fibers, R206L, T204E, and R206L+T204E decreased c significantly by ≈21% (P<0.001), ≈33% (P<0.001), and ≈42% (P<0.001), respectively (Figure 6B). In β-MHC fibers, although none of the TnT variants affected c, the ≈22% (P=0.051) and ≈21% (P=0.053) decrease in c by R206L and R206L+T204E, respectively, were close to being significant (Figure 6B). Qualitatively, these observations are similar to what we observed in tension cost experiments, because g decreases in α-MHC+T204E fibers, but that effect is abolished in β-MHC+T204E fibers. Here, again, our data suggest that R206L slows g in both α- and β-MHC fibers, regardless of the influence of T204E. Our observation on the slowing effect of R206L on g is in agreement with an earlier study that tested the effects of R206L against the α-MHC background using in vitro motility assay.[19]

Effects of α- and β-MHC Isoforms on the R206L- and R206L+T204E-Mediated Impact on XB Recruitment Dynamics

To test whether the R206L- and R206L+T204E-mediated effects on XB recruitment dynamics were differentially

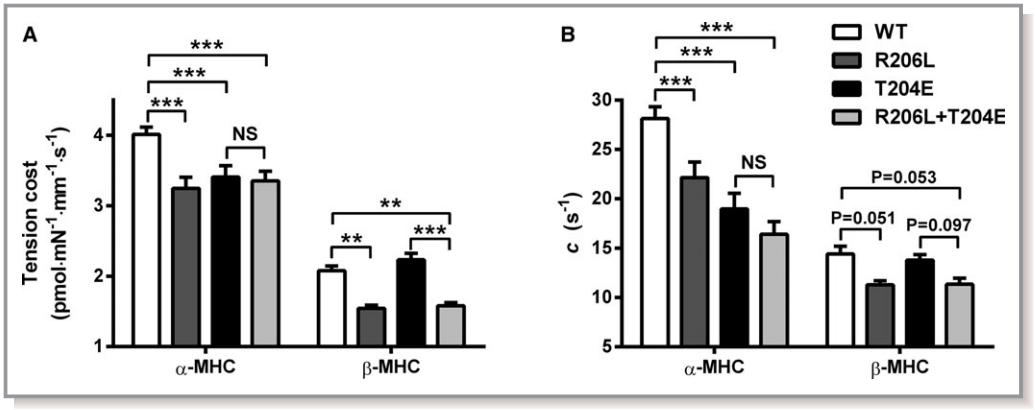

Figure 6. Effects of α- and β-MHC isoforms on the R206L- and R206L+T204E-mediated impact on tension cost and *c*. Both parameters were estimated as described previously.[6] Bar graphs showing the differential impacts of TnT variants on (A) tension cost and (B) *c* in α- and β-MHC fibers. Data were analyzed using 2-way ANOVA, and subsequent post-hoc multiple pair-wise comparisons were made using Fisher's LSD method. Asterisks indicate a statistically significant result when compared to respective control fibers (***P*<0.01; ****P*<0.001; NS). Fibers from 3 normal and 3 PTU-treated rat hearts were used for investigating each of the TnT variants in this study. For tension cost, n=16 for α-MHC+WT, 15 for α-MHC+R206L, 15 for α-MHC+T204E, 17 for α-MHC+R206L+T204E, 14 for β-MHC+WT, 15 for β-MHC+R206L, 19 for β-MHC+T204E, and 16 for β-MHC+R206L+T204E. For *c*, n=16 for α-MHC+WT, 15 for α-MHC+R206L, 15 for α-MHC+T204E, 15 for α-MHC+R206L+T204E, 14 for β-MHC+WT, 15 for β-MHC+R206L, 19 for β-MHC+T204E, and 16 for β-MHC+R206L+T204E. Values are reported as mean±SEM. MHC indicates myosin heavy chain; n, number of fibers in each group; LSD, least significant difference; NS, not significant; PTU, propylthiouracil; TnT, troponin T; WT, wild type.

modulated by α- and β-MHC isoforms, we estimated 2 rate constants that are associated with tension redevelopment (k_{tr}) and XB recruitment dynamics (*b*). k_{tr} denotes the rate constant of recruitment of XBs from the non-force-bearing to force-bearing state and was estimated using a large slack-restretch ML maneuver (Figure 7A and 7B). *b* represents the rate constant of delayed recruitment of additional XBs from the steady-state to new steady state and was estimated using a small, step-like ML change (Figure 1). Two-way ANOVA of k_{tr} revealed a significant interaction effect between MHC isoforms and TnT variants ($P<0.001$), demonstrating a differential impact of α- and β-MHC isoforms on how the TnT variants affected k_{tr}. Post-hoc multiple pair-wise comparisons revealed the following: In α-MHC fibers, T204E attenuated k_{tr} by ≈35% in ($P<0.001$; Figure 7C), but it was unaffected by R206L and R206L+T204E. It is interesting to note that R206L negated the attenuating effect of T204E on k_{tr} because of the cumulative effect of R206L+T204E in α-MHC fibers (Figure 7C). In β-MHC fibers, k_{tr} was not altered by any of the TnT variants. Our observations from k_{tr} experiments were substantiated by our estimates of *b*, which showed a similar trend. Two-way ANOVA of *b* revealed a significant interaction effect ($P<0.001$) between MHC isoforms and the TnT variants. Post-hoc multiple pair-wise comparisons revealed that T204E decreased *b* by ≈27% in α-MHC fibers ($P<0.001$; Figure 7D), but not in β-MHC fibers. In both α- and β-MHC fibers, *b* was unaffected by R206L and R206L+T204E. Conclusions drawn from these 2 independent experiments show that although R206L does not alter XB recruitment dynamics by itself, it abolishes the attenuating effects of T204E on XB recruitment dynamics, regardless of the MHC isoform.

Discussion

We have recently demonstrated that the interplay between the PKC phosphomimic of TnT (T204E)- and MHC isoform-mediated effects bring about different functional states of cardiac thin filaments.[6] Interestingly, T204E and a DCM-linked TnT mutation (R206L) are adjacent to each other, within the H1-helix of TnT. Therefore, we posited that the effect of R206L is also altered differentially by MHC isoforms and that such effects are further modulated by T204E. For the very first time (to our knowledge), we have demonstrated that the contractile dysfunction arising from a DCM-linked TnT mutation (R206L) is not only modulated differently by α- and β-MHC, but may also be exacerbated by a PTM of TnT.

β-MHC, but Not α-MHC, Has a Negating Effect on Attenuation of Tension Mediated by R206L and T204E

A major finding was that α- and β-MHC isoforms differently affected the R206L-mediated impact on Ca^{2+}-activated

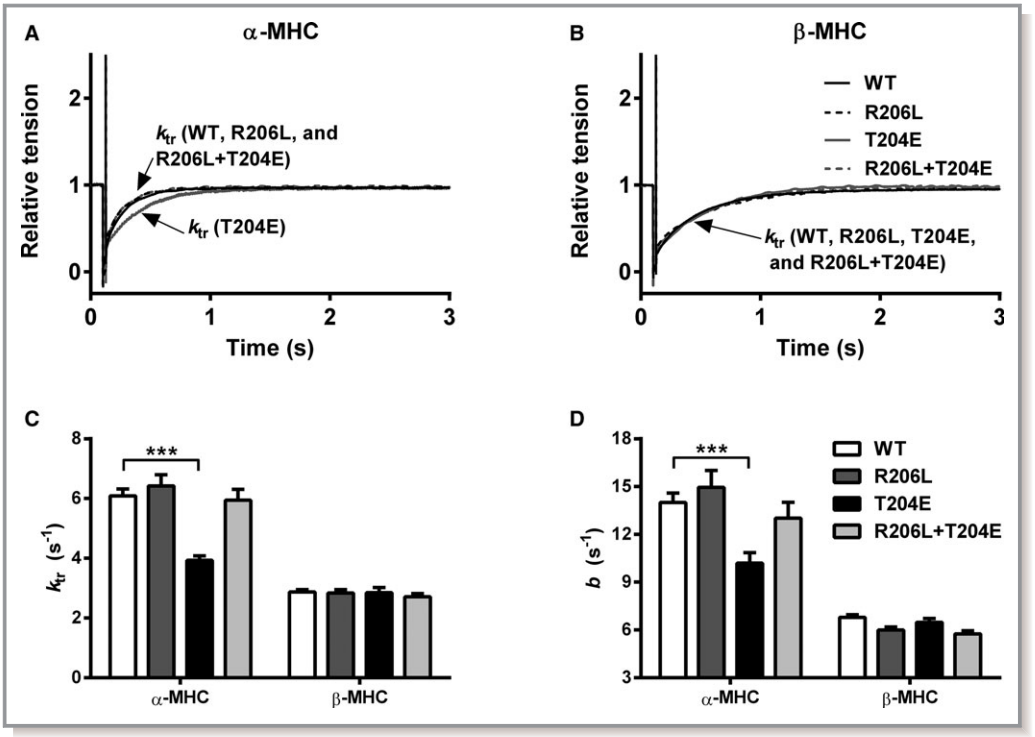

Figure 7. Effects of α- and β-MHC isoforms on the R206L- and R206L+T204E-mediated impact on k_{tr} and *b*. k_{tr} was estimated at pCa 4.3 using a rapid release/restretch protocol, as described in the Materials and Methods. Representative traces of normalized force responses from reconstituted (A) α- and (B) β-MHC fibers. We estimated *b* as described in the Materials and Methods. Bar graph showing the differential impacts of TnT variants on (C) k_{tr} and (D) *b* in α- and β-MHC fibers. Data were analyzed using 2-way ANOVA, and subsequent post-hoc multiple pair-wise comparisons were made using Fisher's LSD method. Asterisks indicate a statistically significant result when compared to respective control fibers (***P<0.001). Fibers from 3 normal and 3 PTU-treated rat hearts were used for investigating each of the TnT variants in this study. For k_{tr}, n=16 for α-MHC+WT, 15 for α-MHC+R206L, 15 for α-MHC+T204E, 14 for α-MHC+R206L+T204E, 14 for β-MHC+WT, 15 for β-MHC+R206L, 19 for β-MHC+T204E, and 19 for β-MHC+R206L+T204E. For *b*, n=16 for α-MHC+WT, 15 for α-MHC+R206L, 15 for α-MHC+T204E, 15 for α-MHC+R206L+T204E, 14 for β-MHC+WT, 15 for β-MHC+R206L, 19 for β-MHC+T204E, and 16 for β-MHC+R206L+T204E. Values are reported as mean±SEM. MHC indicates myosin heavy chain; n, number of fibers in each group; LSD, least significant difference; PTU, propylthiouracil; TnT, troponin T; WT, wild type.

maximal tension. To elaborate, R206L attenuated the Ca^{2+}-activated maximal tension in α-MHC fibers, but had no effect in β-MHC fibers (Figure 3A). Observations made by 2 earlier studies suggested that R206L attenuated thin-filament activation by decreasing the binding affinity of Ca^{2+} to TnC.[24,25] A decrease in the binding of Ca^{2+} to TnC is expected to attenuate the level of activation of RUs (Tn-Tm), resulting in fewer force-bearing XBs. This postulation was substantiated by our E_D estimates, which demonstrated that the number of force-bearing XBs was decreased in α-MHC+R206L fibers, but not in β-MHC+R206L fibers (Figure 3B). Mechanistic insights into how β-MHC abolished the negative effects of R206L may be gained by considering the slower XB cycling kinetics of β-MHC.[6,9] The slower cycling β-MHC is expected to augment cooperative mechanisms in the thin filament because of its longer XB dwell time in the strongly bound state.

In the presence of T204E, the Ca^{2+}-activated maximal tension decreased in both α-MHC+R206L+T204E and β-MHC+R206L+T204E fibers (Figure 3A). Here, again, we observe that β-MHC counters the negative effect of T204E on thin-filament activation, although not completely. To provide a rational explanation for why β-MHC fails to completely negate the inhibitory effect of R206L+T204E, we must first consider the individual effects of R206L and T204E on activation. The magnitude of inhibition of activation is much more pronounced with T204E than R206L, suggesting that both TnT variants affect thin filament activation by different molecular mechanisms. As explained earlier, R206L may decrease binding of Ca^{2+} to TnC, thereby attenuating RU activation. On the other hand, T204E may alter TnC-TnI interactions to attenuate the spread of the Ca^{2+}-mediated signal from the Tn core domain to the tail domain and Tm.[14] Based on these observations, we

posit that the additional downstream impact of T204E on TnC-TnI[44] and Tn-Tm interactions may minimize the rescuing effects of β-MHC on thin-filament activation. This notion is substantiated by 2 experimental observations in this study: (1) The magnitude of Ca^{2+}-desensitization of myofilaments is greater in β-MHC+R206L+T204E fibers (≈0.25 pCa units; $P<0.001$) versus β-MHC+R206L fibers (≈0.05 pCa units; $P<0.05$; Figure 4C); and (2) the magnitude of attenuation of tension is greater in β-MHC+R206L+T204E fibers (≈40%; $P<0.001$) versus β-MHC+R206L fibers (≈4%; statistically insignificant; Figure 3A).

In addition to the negating effects of β-MHC on attenuation of tension by R206L and T204E, our tension estimates led us to another interesting observation. While there was no difference between tensions of α-MHC+T204E and α-MHC+R206L+T204E fibers, tensions of β-MHC+R206L+T204E fibers were ≈11% lower than β-MHC+T204E fibers (Figure 3A). These observations suggest that interplay between the effects mediated by β-MHC, R206L, and T204E exacerbates the attenuation in tension, although β-MHC counteracts the attenuation of tension mediated by either R206L or T204E. Although the myofilament Ca^{2+} sensitivity decreases to a similar extent in β-MHC+T204E and β-MHC+R206L+T204E fibers (Figure 4C), the attenuation of tension is greater in β-MHC+R206L+T204E fibers (Figure 3A). Significant decreases in n_H suggests that myofilament cooperativity is attenuated in β-MHC+R206L+T204E fibers (Figure 5A). Therefore, we posit that the greater attenuation of tension in β-MHC+R206L+T204E fibers results from the attenuated myofilament Ca^{2+} sensitivity (Figure 4C) and cooperativity (Figure 5A).

R206L-Mediated Effects on XB Cycling Kinetics are Independent of the Effects Mediated by MHC Isoforms and T204E

R206L decreased the rate of XB detachment (g), as indicated by the decrease in tension cost (Figure 6A) and c (Figure 6B) in both α- and β-MHC fibers, with and without T204E. Two interesting points to highlight in Figure 6A and 6B are as follows: (1) T204E attenuates g in α-MHC+T204E fibers, but β-MHC negates the attenuating effect of T204E on g in β-MHC+T204E fibers; and (2) R206L over-rides the influence of β-MHC on g, in β-MHC+R206L and β-MHC+R206L+T204E fibers, to exert its negative effect on g. Collectively, these observations suggest that R206L and T204E exert their influence on g by different molecular pathways that interact differently with α- and β-MHC-mediated effects in the thin filament.

R206L did not alter XB turnover kinetics because both k_{tr} (Figure 7C) and b (Figure 7D) were unaffected in α- and β-MHC fibers. This was quite surprising, given the attenuating effect of R206L on g (Figure 6). Generally, a decrease in g alone could attenuate k_{tr} because in a simple 2-state model, $k_{tr} \approx f+g$, where f and g represent the rates of XB attachment and detachment, respectively.[45] However, our data showed that both k_{tr} and b remained unaltered, suggesting a discrepancy between our observations on g and the XB recruitment rates. However, this apparent discrepancy may be resolved by considering that f plays a much greater influence than g on k_{tr}[46,47]; therefore, a slight decrease in g need not result in a decrease in k_{tr}. Two other important observations to note from our estimates of XB recruitment dynamics are: (1) T204E decreased both k_{tr} (Figure 7C) and b (Figure 7D) in α-MHC+T204E fibers, but not in β-MHC+T204E fibers, demonstrating that β-MHC over-rides the influence of T204E on XB recruitment dynamics; and (2) in α-MHC+T204E+R206L fibers, both k_{tr} (Figure 7C) and b (Figure 7D) were unaltered, which suggests that R206L negates the attenuating effect of T204E on XB turnover rates in α-MHC fibers. This finding also suggests different modes of mechanisms for R206L and T204E on XB cycling kinetics.

Interplay Between β-MHC-, T204E-, and R206L-Mediated Effects on the Thin Filament Impairs LDA

Another interesting observation from our study was that E_R, an index of LDA,[35,48,49] was attenuated only in β-MHC+R206L+T204E fibers (Figure 5B). In order to understand how an interplay between β-MHC-, T204E-, and R206L-mediated effects on the thin filament impairs LDA, we consider the 2 factors implicated in its regulation: the extent of Ca^{2+}-mediated activation of the myofilament before the stretch and the cooperative recruitment of force-bearing XBs after the stretch.[48,50] Our data suggests that myofilament activation before the stretch was attenuated, because maximal tension was decreased in β-MHC+R206L+T204E fibers (Figure 3A). It is also likely that cooperative processes mediating recruitment of XBs are impaired because n_H was also decreased in β-MHC+R206L+T204E fibers (Figure 5A). Therefore, we reason that the collective effects of R206L and T204E blunt mechanisms that underlie LDA in β-MHC fibers by attenuating cooperative processes involved in activation of the myofilament.

Summary and Conclusion

The R206L-mediated effects on Ca^{2+}-activated tension in α-MHC fibers suggest a relatively severe effect on the cardiac phenotype, rather than a subtle phenotype that we observed in β-MHC fibers. Attenuated Ca^{2+} sensitivity—as we observed in β-MHC fibers—has been previously linked to decrease in ejection fraction, elevated ventricular volume, increase in

preload, chronic stretching of the muscle, and dilation of ventricles.[2,8] The relatively severe effects on tension in α-MHC fibers is likely to affect the human heart more prominently during the neonatal stages[51,52]; however, the available clinical data on humans reveals a different story.[1] For instance, severity among the affected individuals varied significantly. For example, the proband received a cardiac transplant at the age of 16 years, but her younger sister died of cardiac failure at the age of 20 years. Their mother, who was also affected with DCM, was alive at age 48 years, whereas the maternal grandmother succumbed to an inexplicably sudden death at age 24 years. Collectively, these observations are strongly suggestive of 2 important points: (1) Cardiac functional abnormality in humans is unlikely to be as severe as the studies on α-MHC fibers suggest; and (2) varied severity among individuals suggests the involvement of other additional factors that exacerbate the progression of disease in some individuals. One such additional factor could be the PKC-mediated phosphorylation of myofilament targets, such as TnT (T204E), because several PKC isoforms are upregulated in failing human hearts.[16,17] While this remains to be substantiated in humans,[18] 2 independent rodent studies have shown an increased phosphorylation of TnT residue T204, during cardiac pathology: (1) transgenic mice carrying K210Δ, a DCM-linked TnT deletion mutation[12] and (2) congestive heart failure rat models.[53] In this regard, our tension estimates suggest that the PKC-mediated phosphorylation of TnT could lead to an exacerbated systolic dysfunction in human patients carrying the R206L mutation. Our E_R estimates also suggest that, because of impaired LDA in such patients, the heart would be unable to match the cardiac output to changes in hemodynamic demands. Because our studies were carried out under conditions that mimicked a fully phosphorylated state of myofilaments, it is possible that the outcome may differ when the level of TnT phosphorylation varies under physiological conditions. Whereas this intriguing possibility remains to be addressed in future studies, our study offers substantial evidence for the interplay between R206L- and TnT phosphorylation-mediated effects on contractile function.

Acknowledgment

The authors sincerely thank Dr. Sampath K. Gollapudi for critically reading the manuscript and offering his suggestions.

Sources of Funding

This work was supported by a grant from the National Heart, Lung, and Blood Institute (Grant No. R01-HL-075643; to Chandra) and a Poncin Fellowship (to Michael).

Disclosures

None.

References

1. Mogensen J, Murphy RT, Shaw T, Bahl A, Redwood C, Watkins H, Burke M, Elliott PM, McKenna WJ. Severe disease expression of cardiac troponin C and T mutations in patients with idiopathic dilated cardiomyopathy. *J Am Coll Cardiol*. 2004;44:2033–2040.
2. Du CK, Morimoto S, Nishii K, Minakami R, Ohta M, Tadano N, Lu QW, Wang YY, Zhan DY, Mochizuki M, Kita S, Miwa Y, Takahashi-Yanaga F, Iwamoto T, Ohtsuki I, Sasaguri T. Knock-in mouse model of dilated cardiomyopathy caused by troponin mutation. *Circ Res*. 2007;101:185–194.
3. Hershberger RE, Pinto JR, Parks SB, Kushner JD, Li D, Ludwigsen S, Cowan J, Morales A, Parvatiyar MS, Potter JD. Clinical and functional characterization of TNNT2 mutations identified in patients with dilated cardiomyopathy. *Circ Cardiovasc Genet*. 2009;2:306–313.
4. Van Acker H, De Sutter J, Vandekerckhove K, de Ravel TJ, Verhaaren H, De Backer J. Dilated cardiomyopathy caused by a novel TNNT2 mutation-added value of genetic testing in the correct identification of affected subjects. *Int J Cardiol*. 2010;144:307–309.
5. Michael JJ, Chandra M. Functional effects of the H1-helix of rat cardiac troponin T on crossbridge detachment rate is differently modulated by α- and ß-myosin heavy chain isoforms. *Biophys J*. 2015;108:p596a Abstract.
6. Michael JJ, Gollapudi SK, Chandra M. Effects of pseudo-phosphorylated rat cardiac troponin T are differently modulated by α- and β-myosin heavy chain isoforms. *Basic Res Cardiol*. 2014;109:442.
7. Gollapudi SK, Chandra M. The effect of cardiomyopathy mutation (R97 I) in mouse cardiac troponin T on the muscle length-mediated recruitment of crossbridges is modified divergently by α- and β-myosin heavy chain. *Arch Biochem Biophys*. 2016; pii: S0003-9861(16)30008-X. doi: 10.1016/j.abb.2016.01.008. [Epub ahead of print].
8. Gollapudi SK, Tardiff JC, Chandra M. The functional effect of dilated cardiomyopathy mutation (R144W) in mouse cardiac troponin T is differently affected by α- and β-myosin heavy chain isoforms. *Am J Physiol Heart Circ Physiol*. 2015;308:H884–H893.
9. Mamidi R, Chandra M. Divergent effects of α- and β-myosin heavy chain isoforms on the N terminus of rat cardiac troponin T. *J Gen Physiol*. 2013;142:413–423.
10. Chandra V, Gollapudi SK, Chandra M. Rat cardiac troponin t mutation (F72L)-mediated impact on thin filament cooperativity is divergently modulated by α- and β-myosin heavy chain isoforms. *Am J Physiol Heart Circ Physiol*. 2015;309:H1260–H1270. doi:10.1152/ajpheart.00519.2015.
11. Michael JJ, Tal L, Tardiff JC, Chandra M. Pseudophosphorylation of cardiac troponin I residues 23/24 decreases myofilament Ca^{2+} sensitivity in transgenic mice containing D230N mutation in α-tropomyosin. *Biophys J*. 2013;104:p482a Abstract
12. Sfichi-Duke L, Garcia-Cazarin ML, Sumandea CA, Sievert GA, Balke CW, Zhan DY, Morimoto S, Sumandea MP. Cardiomyopathy-causing deletion K210 in cardiac troponin T alters phosphorylation propensity of sarcomeric proteins. *J Mol Cell Cardiol*. 2010;48:934–942.
13. Jideama NM, Noland TA Jr, Raynor RL, Blobe GC, Fabbro D, Kazanietz MG, Blumberg PM, Hannun YA, Kuo JF. Phosphorylation specificities of protein kinase C isozymes for bovine cardiac troponin I and troponin T and sites within these proteins and regulation of myofilament properties. *J Biol Chem*. 1996;271:23277–23283.
14. Sumandea MP, Pyle WG, Kobayashi T, de Tombe PP, Solaro RJ. Identification of a functionally critical protein kinase C phosphorylation residue of cardiac troponin T. *J Biol Chem*. 2003;278:35135–35144.
15. Sumandea MP, Vahebi S, Sumandea CA, Garcia-Cazarin ML, Staidle J, Homsher E. Impact of cardiac troponin T N-terminal deletion and phosphorylation on myofilament function. *Biochemistry*. 2009;48:7722–7731.
16. Bowling N, Walsh RA, Song G, Estridge T, Sandusky GE, Fouts RL, Mintze K, Pickard T, Roden R, Bristow MR, Sabbah HN, Mizrahi JL, Gromo G, King GL, Vlahos CJ. Increased protein kinase C activity and expression of Ca^{2+}-sensitive isoforms in the failing human heart. *Circulation*. 1999;99:384–391.
17. Simonis G, Briem SK, Schoen SP, Bock M, Marquetant R, Strasser RH. Protein kinase C in the human heart: differential regulation of the isoforms in aortic stenosis or dilated cardiomyopathy. *Mol Cell Biochem*. 2007;305:103–111.
18. Streng AS, de Boer D, van der Velden J, van Dieijen-Visser MP, Wodzig WK. Posttranslational modifications of cardiac troponin T: an overview. *J Mol Cell Cardiol*. 2013;63:47–56.

19. Mirza M, Marston S, Willott R, Ashley C, Mogensen J, McKenna W, Robinson P, Redwood C, Watkins H. Dilated cardiomyopathy mutations in three thin filament regulatory proteins result in a common functional phenotype. *J Biol Chem*. 2005;280:28498–28506.
20. Hunter JC, Korzick DH. Age- and sex-dependent alterations in protein kinase C (PKC) and extracellular regulated kinase 1/2 (ERK1/2) in rat myocardium. *Mech Ageing Dev*. 2005;126:535–550.
21. Towbin JA, Solaro RJ. Genetics of dilated cardiomyopathy: more genes that kill. *J Am Coll Cardiol*. 2004;44:2041–2043.
22. Takeda S, Yamashita A, Maeda K, Maeda Y. Structure of the core domain of human cardiac troponin in the $Ca^{(2+)}$-saturated form. *Nature*. 2003;424:35–41.
23. Jin JP, Chong SM. Localization of the two tropomyosin-binding sites of troponin T. *Arch Biochem Biophys*. 2010;500:144–150.
24. Kobayashi M, Debold EP, Turner MA, Kobayashi T. Cardiac muscle activation blunted by a mutation to the regulatory component, troponin T. *J Biol Chem*. 2013;288:26335–26349.
25. Robinson P, Griffiths PJ, Watkins H, Redwood CS. Dilated and hypertrophic cardiomyopathy mutations in troponin and α-tropomyosin have opposing effects on the calcium affinity of cardiac thin filaments. *Circ Res*. 2007;101:1266–1273.
26. Inoue T, Kobirumaki-Shimozawa F, Kagemoto T, Fujii T, Terui T, Kusakari Y, Hongo K, Morimoto S, Ohtsuki I, Hashimoto K, Fukuda N. Depressed Frank-Starling mechanism in the left ventricular muscle of the knock-in mouse model of dilated cardiomyopathy with troponin T deletion mutation δK210. *J Mol Cell Cardiol*. 2013;63:69–78.
27. Chandra M, Tschirgi ML, Rajapakse I, Campbell KB. Troponin T modulates sarcomere length-dependent recruitment of cross-bridges in cardiac muscle. *Biophys J*. 2006;90:2867–2876.
28. Pan BS, Johnson RG Jr. Interaction of cardiotonic thiadiazinone derivatives with cardiac troponin C. *J Biol Chem*. 1996;271:817–823.
29. Guo X, Wattanapermpool J, Palmiter KA, Murphy AM, Solaro RJ. Mutagenesis of cardiac troponin I. Role of the unique NH2-terminal peptide in myofilament activation. *J Biol Chem*. 1994;269:15210–15216.
30. Tardiff JC, Factor SM, Tompkins BD, Hewett TE, Palmer BM, Moore RL, Schwartz S, Robbins J, Leinwand LA. A truncated cardiac troponin T molecule in transgenic mice suggests multiple cellular mechanisms for familial hypertrophic cardiomyopathy. *J Clin Invest*. 1998;101:2800–2811.
31. Chandra M, Tschirgi ML, Ford SJ, Slinker BK, Campbell KB. Interaction between myosin heavy chain and troponin isoforms modulate cardiac myofiber contractile dynamics. *Am J Physiol Regul Integr Comp Physiol*. 2007;293:R1595–R1607.
32. Mamidi R, Michael JJ, Muthuchamy M, Chandra M. Interplay between the overlapping ends of tropomyosin and the N terminus of cardiac troponin T affects tropomyosin states on actin. *FASEB J*. 2013;27:3848–3859.
33. Gollapudi SK, Mamidi R, Mallampalli SL, Chandra M. The N-terminal extension of cardiac troponin T stabilizes the blocked state of cardiac thin filament. *Biophys J*. 2012;103:940–948.
34. Fabiato A, Fabiato F. Calculator programs for computing the composition of the solutions containing multiple metals and ligands used for experiments in skinned muscle cells. *J Physiol (Paris)*. 1979;75:463–505.
35. Ford SJ, Chandra M, Mamidi R, Dong W, Campbell KB. Model representation of the nonlinear step response in cardiac muscle. *J Gen Physiol*. 2010;136:159–177.
36. Campbell KB, Chandra M, Kirkpatrick RD, Slinker BK, Hunter WC. Interpreting cardiac muscle force-length dynamics using a novel functional model. *Am J Physiol Heart Circ Physiol*. 2004;286:H1535–H1545.
37. Michael JJ, Gollapudi SK, Ford SJ, Kazmierczak K, Szczesna-Cordary D, Chandra M. Deletion of 1-43 amino acids in cardiac myosin essential light chain blunts length dependency of $Ca^{(2+)}$ sensitivity and cross-bridge detachment kinetics. *Am J Physiol Heart Circ Physiol*. 2013;304:H253–H259.
38. Brenner B, Eisenberg E. Rate of force generation in muscle: correlation with actomyosin atpase activity in solution. *Proc Natl Acad Sci USA*. 1986;83:3542–3546.
39. Fitzsimons DP, Patel JR, Moss RL. Role of myosin heavy chain composition in kinetics of force development and relaxation in rat myocardium. *J Physiol*. 1998;513(Pt 1):171–183.
40. Herron TJ, Korte FS, McDonald KS. Loaded shortening and power output in cardiac myocytes are dependent on myosin heavy chain isoform expression. *Am J Physiol Heart Circ Physiol*. 2001;281:H1217–H1222.
41. Metzger JM, Wahr PA, Michele DE, Albayya F, Westfall MV. Effects of myosin heavy chain isoform switching on Ca^{2+}-activated tension development in single adult cardiac myocytes. *Circ Res*. 1999;84:1310–1317.
42. Gordon AM, Homsher E, Regnier M. Regulation of contraction in striated muscle. *Physiol Rev*. 2000;80:853–924.
43. Huxley AF. Muscle structure and theories of contraction. *Prog Biophys Biophys Chem*. 1957;7:255–318.
44. Schlecht W, Zhou Z, Li KL, Rieck D, Ouyang Y, Dong WJ. FRET study of the structural and kinetic effects of PKC phosphomimetic cardiac troponin T mutants on thin filament regulation. *Arch Biochem Biophys*. 2014;550–551:1–11.
45. Brenner B. Effect of Ca2+ on cross-bridge turnover kinetics in skinned single rabbit psoas fibers: implications for regulation of muscle contraction. *Proc Natl Acad Sci USA*. 1988;85:3265–3269.
46. de Tombe PP, Stienen GJ. Impact of temperature on cross-bridge cycling kinetics in rat myocardium. *J Physiol*. 2007;584:591–600.
47. Ford SJ, Chandra M. The effects of slow skeletal troponin I expression in the murine myocardium are influenced by development-related shifts in myosin heavy chain isoform. *J Physiol*. 2012;590:6047–6063.
48. Stelzer JE, Larsson L, Fitzsimons DP, Moss RL. Activation dependence of stretch activation in mouse skinned myocardium: implications for ventricular function. *J Gen Physiol*. 2006;127:95–107.
49. Mamidi R, Mallampalli SL, Wieczorek DF, Chandra M. Identification of two new regions in the N-terminal region of cardiac troponin T that have divergent effects on cardiac contractile function. *J Physiol*. 2013;591:1217–1234.
50. Campbell KB, Chandra M. Functions of stretch activation in heart muscle. *J Gen Physiol*. 2006;127:89–94.
51. Bouvagnet P, Neveu S, Montoya M, Leger JJ. Development changes in the human cardiac isomyosin distribution: an immunohistochemical study using monoclonal antibodies. *Circ Res*. 1987;61:329–336.
52. Wessels A, Mijnders TA, de Gier-de Vries C, Vermeulen JLM, Vir'gh S, Lamers WH, Moorman AFM. Expression of myosin heavy chain in neonatal human hearts. *Cardiol Young*. 1992;2:318–334.
53. Belin RJ, Sumandea MP, Sievert GA, Harvey LA, Geenen DL, Solaro RJ, de Tombe PP. Interventricular differences in myofilament function in experimental congestive heart failure. *Pflugers Arch*. 2011;462:795–809.